UCRL-JRNL-237027

LAWRENCE
LIVERMORE
NATIONAL
LABORATORY

Discrete Element Modeling

J. Morris, S. Johnson

December 5, 2007

American Society of Civil Engineers: Journal of Geotechnical and Geoenvironmental Engineering

Discrete Element Modeling

Overview:

The Distinct Element Method (also frequently referred to as the Discrete Element Method) (DEM) is a Lagrangian numerical technique where the computational domain consists of discrete solid elements which interact via compliant contacts. This can be contrasted with Finite Element Methods where the computational domain is assumed to represent a continuum (although many modern implementations of the FEM can accommodate some Distinct Element capabilities). Often the terms Discrete Element Method and Distinct Element Method are used interchangeably in the literature, although Cundall and Hart (1992) suggested that Discrete Element Methods should be a more inclusive term covering Distinct Element Methods, Displacement Discontinuity Analysis and Modal Methods. In this work, DEM specifically refers to the Distinct Element Method, where the discrete elements interact via *compliant contacts*, in contrast with Displacement Discontinuity Analysis where the *contacts are rigid* and all compliance is taken up by the adjacent intact material.
A theoretical basis for the DEM is provided by Williams et. al (1985). A key aspect of the technique is that it can simulate many objects interacting even when the topology of the arrangement is entirely changed. Consequently, DEM research has involved optimization of nearest neighbor sorting algorithms (see Williams and O'Conner, 1995; Munjiza et al, 1993; Perkins and Williams, 2001; Perkins and Williams, 2002; Munjiza and Andrews, 1998). The DEM solves Newton's equations of motion to resolve particle motion and adds a contact law to resolve inter-particle contact forces. Forces are typically integrated explicitly in time to acquire the time history response of the material using an appropriate quadrature method. A 2^{nd} order accurate method is usually sufficient and has been shown to be optimal in terms of total simulation time under several circumstances (Rougier et al, 2004). The DEM includes a family of techniques that use radically different treatments for the element geometry and the form of the contact forces. This discussion documents the various forms of DEM employed and the applications typically considered.

Early approaches to the DEM employed rigid disks or spheres with compliant contacts (Cundall and Strack, 1979).. These approaches have the advantage that the algorithms for detecting contact and calculating forces between particles are relatively straight forward. However, they are not appropriate for representing all discrete media. For example, to closely mimic tight rock structures, Cundall (1980), Walton (1980) and Cundall and Hart (1985) developed two-dimensional DEMs that employed arbitrary polygons. These approaches were later extended to 3-dimensions by Cundall (1988) and Hart et al. (1988) who developed DEMs composed of rigid and deformable polyhedral blocks with compliant contacts. In order to simplify contact resolution between polyhedral blocks, Cundall (1988) developed the common plane approach which rapidly and interatively identifies the area of overlap between the polyhedra.

Contact in DEM is captured through a "soft object" model, where interpenetration of the objects is allowed and interpreted physically as local elasto-plastic deformation of the object at the contact surface. To capture the response of the material at the contact points, a variety of contact laws have been proposed, from simple linear to highly non-linear forms. An overview of contact models for granular applications of the 2-D and 3-D DEM can be found in Walton (1994) and Luding (2006).

For jointed rock numerous models have been developed for the DEM. It is worth mentioning that such models are required to not simply reproduce data, but also be suitable for inclusion in a numerical method. These issues are discussed in detail by Morris (2003). Models have been developed for the DEM which include non-linear, hysteretic load-unload paths in the normal response of the joint and dilation in shear. The most sophisticated of these models have been demonstrated to reproduce a wide range of experimental data for joints in a variety of materials and yet be numerically robust. These approaches typically take estimates of the normal and shear displacement increments on a joint at each timestep and use them to integrate the normal and shear stress on the joint subject to limitations such as friction angle. Softening is typically accommodated by allowing the friction angle to change as the joint slips. Dilation is addressed by allowing the normal stress to be affected by the shear displacement (for example, Souley (1995) or Itasca's 3DEC).

DEM has been extended to include the internal stress state of the objects using several different treatments. When appropriate, rigid bodies are preferred because they permit large timesteps to be used. The addition of an internal deformation mode adds computational overhead to each step and requires shorter timesteps for stability of the DEM. Modal dynamics (Williams and Mustoe, 1987; Pentland and Williams, 1989) elements allow selection of modally decoupled deformation modes to tailor the deformation response in a computationally efficient manner. Cosserat points (Rubin, 2001; Morris et al, 2003) provide a non-linear, homogeneously deformable element. Full finite element discretization (Morris et al., 2006; Block et al., 2007) of individual discrete elements is also an option when wavelengths comparable to or shorter than the length of the elements must be resolved. Knowledge of the internal stress state can help to establish criteria for fracturing and fragmenting the individual objects (Owen et al, 2002; Munjiza and Latham, 2002; Morris et al., 2006; Morris and Johnson, 2007). Finite difference (Cundall (1980; 1988) and Hart *et al.* (1988)) can also be used to model the deformation of compliant blocks.

It is possible to develop combined rigid, uniformly deformable, and finite element discretizations within a single framework. For example,.Morris *et al.* (2004), observed that the theory of Cosserat points (Rubin, 1995; 2000) could model each element as a homogenously deformable continuum. A Cosserat point describes the dynamic response of the polyhedral rock block by enforcing a balance of linear momentum to determine the motion of the center of mass (3 translational degrees of freedom), as well as three vector balance laws of director momentum to determine a triad of deformable vectors, which model both the orientation of the element (3 rotational degrees of freedom) and its deformation (6 degrees of freedom for dilatation and distortion). The response of the deformable polyhedral block is modeled explicitly using the standard material constants that characterize the original three-dimensional material, and constitutive equations for the contact forces at the joints become pure measures of the mechanics of joints. This deficiency was overcome by internally discretizing the polyhedral blocks with a collection of smaller tetrahedral elements. The numerical solution procedure depends on nodal balance laws to determine the motion of the four nodes of each tetrahedral element, similar to that described above for the motion of blocks. In general, the accelerations of the nodes of a particular element are coupled with the nodes of the neighboring elements. However, the director inertia coefficients in the theory of a Cosserat point can be specified so that these equations become uncoupled. This form corresponds to a lumped mass assumption and is particularly convenient for wave propagation problems using explicit integration schemes because it does not require the inversion of a stiffness matrix. In continuum regions, where the nodes of neighboring elements are forced to remain common (i.e., unbreakable), the Cosserat point formulation is basically the same as standard finite element models (FEM) that use homogeneously deformable tetrahedral elements. In this case, the computational effort in LDEC is significantly reduced: many nodes are shared and there is no need for contact detection on shared element surfaces. While standard finite element formulations are based on shape functions and weighting functions, the latest version of LDEC utilizes balance laws for the directors of each Cosserat point (associated with the positions of the nodes of the tetrahedral elements). LDEC can be run simultaneously in DEM and FEM-like modes, dynamically blending continuum and discrete regions, as necessary.

Even in the case of rigid elements with deformable contacts it is possible to develop criteria for element breakage. Experimentally-derived tabular approaches have been developed to relate resultant particle size distribution to the energy of impact (Herbst and Potapov, 2004). However, it is also possible to derive estimations of the average stress state within a DEM element, given the contact forces and body forces within the element. This capability can be used to visualize the stress state within the DEM system or to develop criteria for breaking the DEM elements. For example, the average stress tensor may be calculated using a rigid body formulation (Rubin et al, 2006) of the Cosserat point. Using this approach, fracture is assumed to be instantaneous and is initiated when the mean rigid body stress exceeds some criterion appropriate to the material considered.

The DEM has also been extended to include coupling to computational fluid dynamics (CFD) formulations. For simple one-way coupling, applicable in situations where the solid flow is sparse or interstitial fluids do not significantly contribute, models such as Darcy flow models (Preece et al, 1999; Jensen and Preece, 2000; Klosek, 1997) can be employed. This approach may also be formulated to update the porosity/permeability constants as the porous geometry changes. For two-way fluid-solid coupling, useful where the effects of interstitial fluid cannot be neglected, three techniques are commonly used: Lattice-Boltzmann (L-B), Smooth Particle Hydrodynamics (SPH) and pipe flow models. L-B (Cook et al, 2000; Cook et al, 2003) is an Eulerian approach to modeling fluids, which is coupled to DEM models by mapping DEM solids onto the L-B grid, and establishing the fill ratio of individual cells; this technique is also amenable to parallelization for large problems (O'Conner and Friedrich, 1999). SPH (Monaghan, 1992) is a mesh-free Lagrangian approach that can be easily coupled by enforcing compliance between the DEM solid and Lagrangian integration points located inside of the DEM solid (Potapov et al, 2001; Morris and Johnson, 2007). Pipe flow models (Munjiza et al, 2000) are efficient methods of coupling fluid when the pore network is relatively intransient.

Geotechnical Applications of the DEM:

The DEM methods are collectively appropriate for simulating a wide range of geotechnical applications. Cundall (2001) provides a review of DEM simulations of both granular materials and rock masses. Early applications of the simplest spherical element DEM implementations focused on micro-scale modeling of granular geo-materials, including the response of sands and soils at the microscale. More recent work has extended this approach to include interparticle bonds that mimic the response of rocks at the macroscale. For example, Antonellini and Pollard (1995) simulated the formation of shear bands in sandstone using the DEM. Morgan (1999a, 1999b) applied the DEM to the mechanics of granular shear zones. This class of DEM, often called the Bonded Particle Method, is the topic of section ???.

This section documents polyhedral block implementations of the DEM. These have allowed direct simulation of extensive, heavily fractured rock masses. For example, Heuze et al. (1993) used a 2-D polygonal DEM to analyze explosions in hard rock. When considering complicated geologies, polyhedral block implementations of the DEM provide the fundamental advantage that pre-existing joints in rock can be incorporated into the model directly, and the joints are allowed to undergo large deformation. Detailed joint constitutive models (see Morris (2003) for a review) can also be used to combine experimentally observed fracture properties (such as joint dilation, friction angle, and cohesion) with the DEM approach.

Simulations of underground structures in jointed rock:

Heuze and Morris (2007) provide an extensive overview of the DEM as applied to jointed rock masses. One fundamental advantage of the DEM is that pre-existing joints in rock can be incorporated into a DEM model directly, and the joints are allowed to undergo large deformation. Detailed joint constitutive models (see Morris (2003) for a review) can also be used to combine experimentally observed fracture properties (such as joint dilation, friction angle, and cohesion) with the DEM approach. Combined with modern computing power, the DEM provides an opportunity to directly simulate the behavior of in situ rock masses at a scale not previously possible. Here we cover some of the technical details specific to this application of the DEM and present results obtained using these techniques.

Simulation of an extensive underground facility in fractured rock

Morris et al (2006) performed simulations of an extensive, multi-tunnel facility with the Livermore Distinct Element Code (LDEC). The solution domain spanned 60 m in each direction and encapsulated a generic facility that included several tunnel sections and a lift shaft (see Figure 5). Several geological models were considered as part of this study. In particular, the behavior of regular, persistent joints was compared to the effect of non-persistent (i.e., randomized) joints in the surrounding rock. The rigid block capability was used to model hard rock and to emphasize the role of joint geometries. Figure 6 shows an example of the randomized jointing present in the non-persistent model geology. In both cases discussed here, the joint patterns resulted in typical block sizes of 30 cm. Consequently, each model contained approximately 8 million individual polyhedral rock blocks and approximately 100 million contact elements, making these the largest simulations of this type performed to date. The facilities were subjected to loading corresponding to one kiloton at the surface 50 m above.

Figure 7 compares the velocity fields of the two simulations at 30 ms. Results obtained for the regular, persistent joint set and irregular, non-persistent model differed in several key ways:

- The regular model exhibited strong anisotropy. Since the joints are weak under shear loading, the regular, persistent joint sets tend to channel the waveform, resulting in variations in wavespeed with direction of propagation.
- The irregular model exhibited higher attenuation. Again, because the joints are weak under shear loading, the irregular joint structure results in more plastic deformation on the joints and, consequently, more attenuation.
- Persistent joints allow shear motion along the entire length of the computational domain, resulting in large "chimney" effects above collapsed tunnels sections.
- The irregular model resulted in more diffraction of waves around cavities in the rock mass.

Figure 8 shows two snapshots of the collapse of the largest room within the facility using the non-persistent joint set simulation. While the largest room within the facility has totally collapsed, the narrowest access tunnels experienced minimal damage. The midsize tunnels show a range of damage, with most damage occurring in tunnel sections that contain a junction with another tunnel or lift shaft. This behavior is consistent with the idea that tunnel junctions compromise tunnel strength.

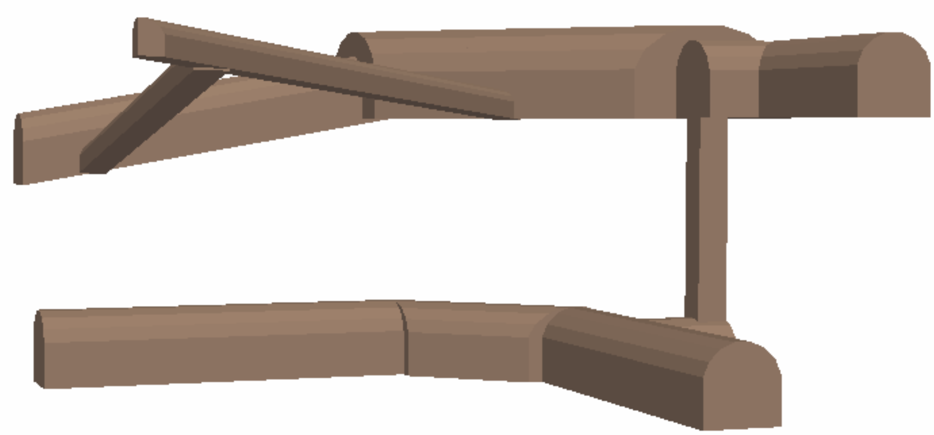

Figure 5: Generic facility model including several tunnel sections and a lift shaft. The facility spans 60m and is 50m below the surface.

Figure 6: The non-persistent randomized geology in the vicinity of one of the tunnels. The near-horizontal joint set persists through the model. However, joint sets in the near vertical direction persist only through several consecutive layers at a time.

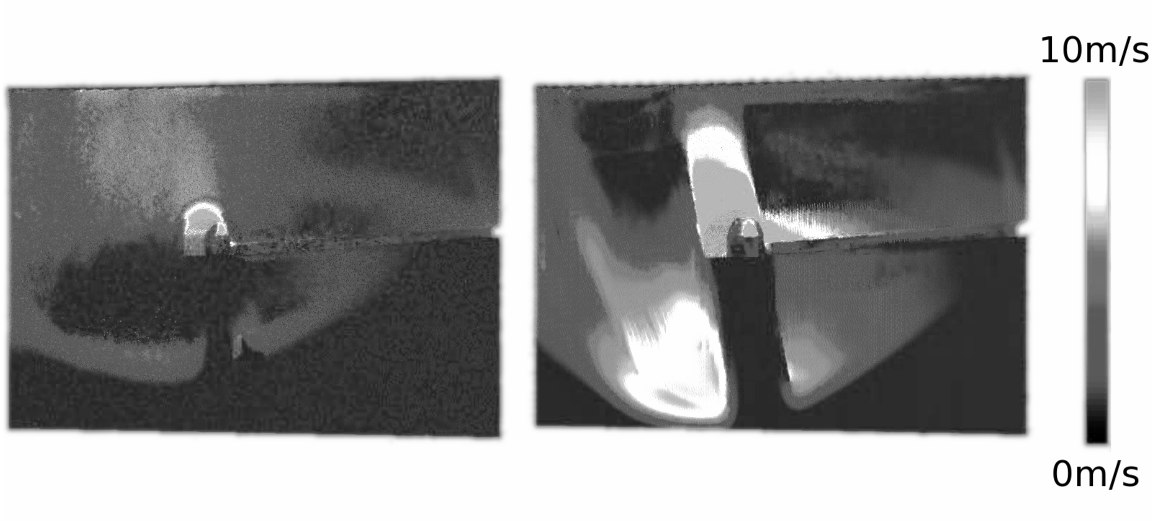

Figure 7: The velocity magnitude for the two models at 30ms. The non-persistent, randomized geology model (left) and regular jointed model (right) exhibit fundamentally different responses to loading.

Figure 8: Snapshots of the largest room at 0 ms and 200 ms, using the non-persistent joint set simulation. The simulation predicts that this large room within the facility would completely collapse under the applied loading.

Simulations of a Tunnel Opening in Infrequently Jointed Rock

The simulation just presented modeled tunnels in heavily jointed, hard rock, where the tunnel diameter was spanned by many blocks. Under such circumstances, it is appropriate to simulate the rock mass using a “tight” structure consisting of polyhedral blocks that are either rigid or homogenously deformable (with deformable points of contact in both cases). In contrast, the focus of this section is on a class of problems where the joints are sufficiently infrequent so that the predominant failure mechanism is block breakage rather than intact rock displacement.

Morris et al (2006) presented a preliminary simulation performed in two dimensions using the LDEC code. The geology consists of blocks of limestone, measuring 1.83 m wide, by 0.30 m high, surrounding a tunnel measuring 2.73 m by 2.80 m. The tunnel is subjected to loading that corresponds to a tamped, one-ton detonation located 4.88 m left and 5.75 m above the tunnel. The calculation was performed in two stages. Initially, LDEC was run with deformable blocks of limestone internally discretized into 10 cm tetrahedral elements. Cohesive elements were not included. In this mode of operation, the time step is quite short so that modes of deformation within the 10 cm elements can be captured. After 10 ms, the LDEC calculation was switched over to rigid-block mode, which ignores internal modes of the elements to increase the size of the time steps and to investigate the flow of rubble into the tunnel over long time scales. The simulation shows that a significant portion of the rock mass surrounding the tunnel is reduced to rubble by the tension produced as waves reflect from the interior surface of the tunnel. This rubble mass is sufficient to fill in the original tunnel.

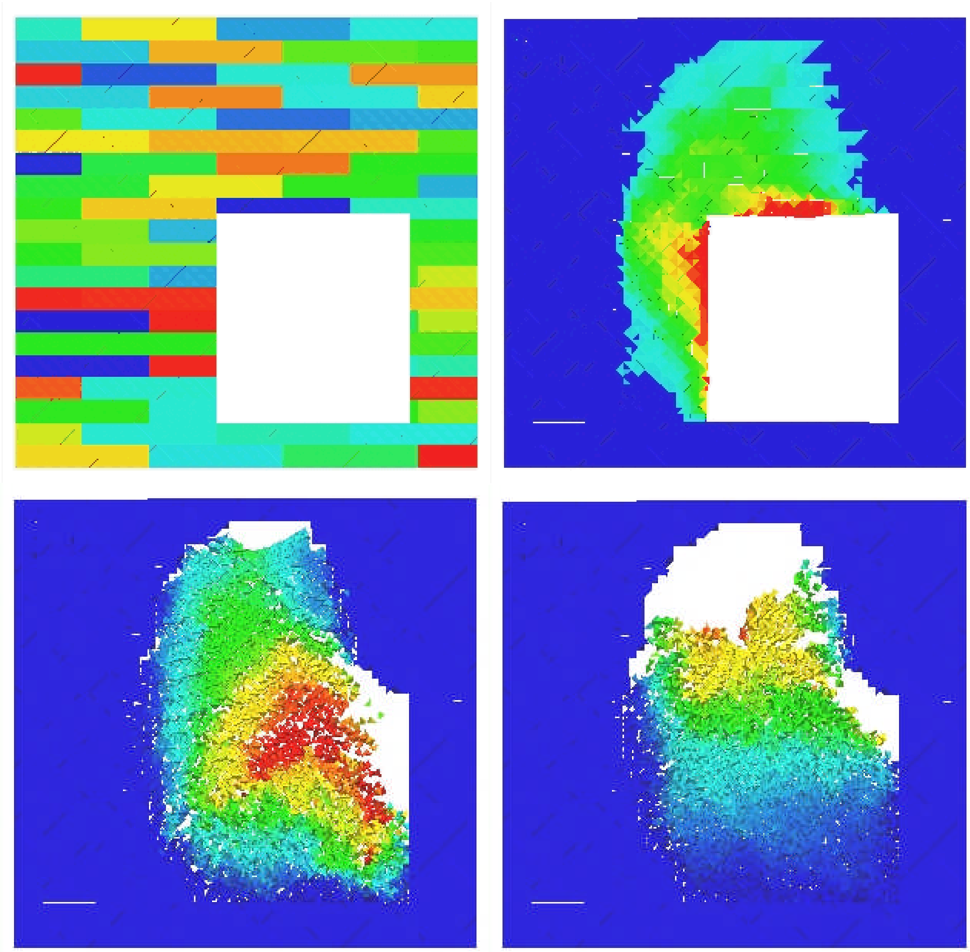

Figure 9: The infrequently jointed model is displayed top left, with individual blocks colored randomly to emphasize joint locations. The simulation results at 10 ms, 500 ms and 1000 ms, show that a significant portion of the surrounding rock is reduced to rubble and fills the tunnel.

Impact into a Boulder Field

The second application of the polyhedral DEM involves interaction between a projectile and a loose pile of polyhedral blocks. A simple and surprisingly effective method of protecting underground targets is through the use of boulder screens, where the boulder diameters are of the same order as the incoming projectile cross-section. Heuze(1989) reviews projectile penetration into geological materials.. Austin et al. (1980, 1981) performed a set of experimental studies on full-scale boulder screens. In addition, small scale, controlled experiments on the mechanics of impact into brittle diorite blocks have been performed (Kumano et al, 1982 and Kumano and Goldsmith 1982). Nelson et al. performed a 2-D DEM analysis of boulder screen performance using cubic and hexagonal lattices of octagonal bodies. Our study focuses on capturing the stochastic, 3-D nature of this system, using polyhedral, orthorhombic, rigid bodies with a fracture and impact point comminution model selected to achieve rapid simulation times.

Two sets of systems were investigated: 1-caliber and 2-caliber boulder fields. Each set of systems consists of 10 separate randomly generated configurations corresponding to the system as measured and described in Austin et al (1980). Each random configuration is produced using a uniform random distribution of dimensions for the orthorhombic bodies, where the product of the dimensions for each body is constrained by volume and aspect ratio limits (taking the maximum or minimum ratio of the set of pairs of orthogonal dimensions within the body). The bodies are rotated randomly about their centroids, placed in a body-centered configuration in layers perpendicular to the gravity potential, and allowed to settle and reorient within a rigid pit of dimensions L20'xH10'xW10'(bottom)11'10"(top).

The fracture criterion was modeled using the mean stress tensor within each body. The stress tensor is calculated using a rigid body formulation (Rubin et al, 2006) of the Cosserat point. Fracture is assumed here to be instantaneous and is initiated when the mean rigid body stress exceeds the von Mises failure criterion. A fracture plane was then introduced in the direction of most principal tensile stress and originating from the point of highest applied force. Comminution at the impact point is approximated as a pyramidal cavity with energy loss due to heat dissipation and surface creation approximated by the release of strain energy in the block before fracture. The cavity model is based on the average equivalent conical cavity geometry derived from data on diorite impact in Kumano1982, which indicates a relatively uniform value of approximately 70-degrees across a range of low speed impacts.

From Figure 2 and Figure 3, it can be seen that the depth of penetration increases with decreasing boulder size. Tthough the homogenized mass fraction and density of the domain remains constantdoes not change, the results indicate a pronounced increase in the penetration of the projectile with decreasing boulder sizechange in the behavior of the projectile. Proportionally less kinetic energy is removed from the projectile during each boulder impact, as both the cross-sectional area and mass of each boulderobject is less in the 1-caliber case (i.e., a factor of 4 and 8, respectively, or 2 and 4 per unit equivalent length of firing path between the two cases) with d. Dissipated energy is converted into kinetic energy of in the resultant boulder-wise ejecta. Especially interesting is the ability of the model to capture j-hooking of the projectile in a granular medium, an observed but poorly understood phenomenon in granular impact.

From Figure 2 and Figure 3, it can be seen that though the homogenized mass fraction and density of the domain remains constant, the results indicate a pronounced increase in the penetration of the projectile with decreasing boulder size. Proportionally less kinetic energy is removed from the projectile during each boulder impact, as both the cross-sectional area and mass of each boulder is less in the 1-caliber case (i.e., a factor of 4 and 8, respectively, or 2 and 4 per unit equivalent length of firing path between the two cases) with dissipated energy converted into kinetic energy in the resultant boulder-wise ejecta. Especially interesting is the ability of the model to capture j-hooking of the projectile in a granular medium, an observed but poorly understood phenomenon in granular impact.

This seminar was sponsored under the auspices of the U.S. Department of Energy by Lawrence Livermore National Laboratory under Contract DE-AC52-07NA27344.

Table 1: Physical properties of diorite

Specific gravity	Modulus of elasticity (psi)	Compressive strength (psi)	Tensile strength (psi)	Nominal dimensions
2.83	5.06e6	3.2e4	2e2	15-18” (1-cal) 30-33” (2-cal)

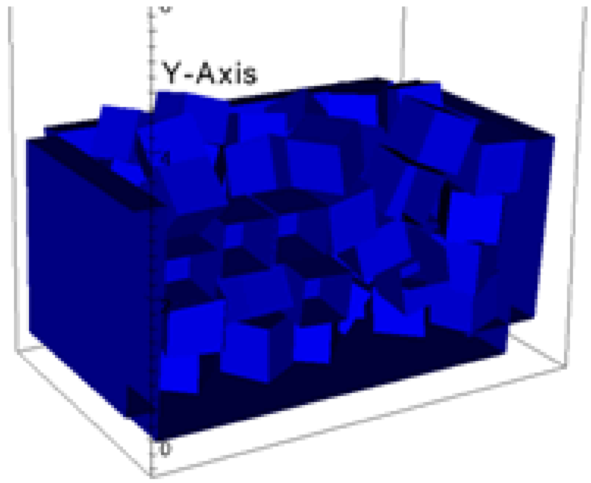

Figure 1: Example of model generation for the boulder shield

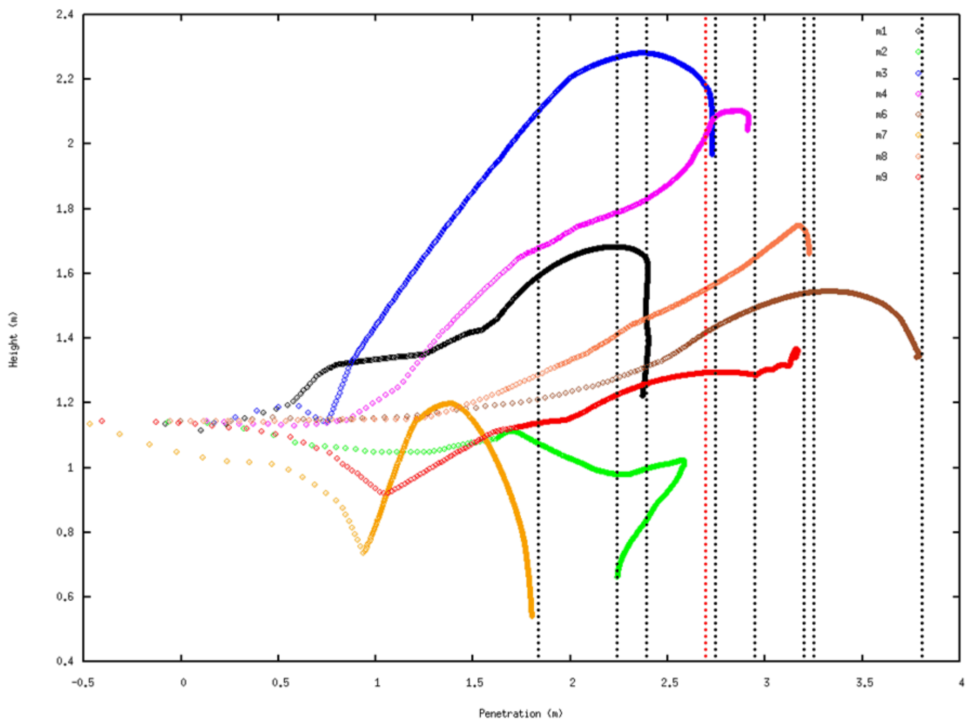

Figure 2: Trajectory tracks for the projectile centroid in 2-caliber boulder field trials projected to the plane of the firing line parallel to gravity

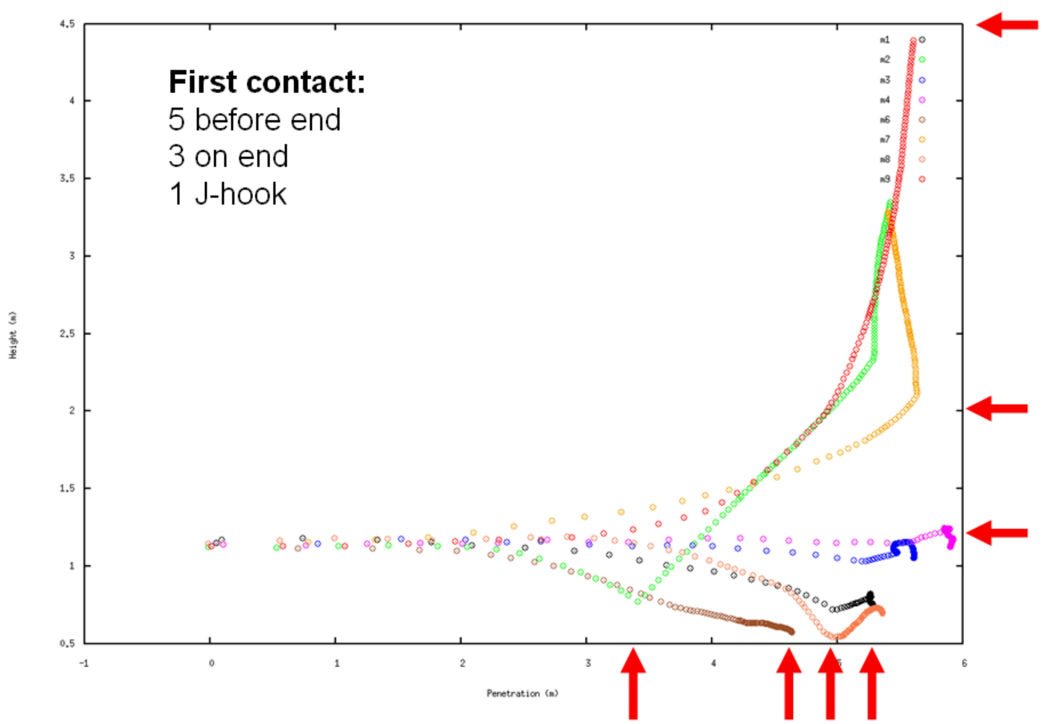

Figure 3: Trajectory tracks for the projectile centroid in 1-caliber boulder field trials projected to the plane of the firing line parallel to gravity

References:

Alder BJ, Wainwright TE. Studies in molecular dynamics. I. General method. *Journal of Chemistry and Physics* 1959; **31**: 459-466

Austin CF, Halsey CC, Berry SL, *Full-scale penetration into semiconfined diorite boulders by a semiarmor-piercing (SAP) bomb and a slender penetrator*, P. W. Department, 'Editor'. 1980, Naval Weapons Center

Austin CF, Halsey CC, Berry SL, *Full-scale penetration into semiconfined diorite boulders by a semiarmor-piercing (SAP) bomb*, D. f. t. Navy, 'Editor'. 1981, Naval Weapons Center: China Lake, California. 27.

Block G, Rubin M, Morris JP. Simulations of dynamic crack propagation in brittle materials using nodal cohesive forces and continuum damage mechanics in the distinct element code LDEC, International Journal of Fracture, 144 (3), 131-147. 2006:

Cook BK, Noble DR, Preece DS, Williams JR, *Direct simulation of particle-laden fluids*. 2000, Sandia National Laboratories: Albuquerque, NM. 11.

Cook BK, Noble D, Williams JR. A direct simulation method for particle-fluid systems. *Engineering Computations* 2003; **21**: 151--168

Cundall, P. A. (1980), UDEC-A generalized distinct element program for modeling jointed rock, Final Tech. Rep. Eur. Res. Office (US Army Contract DAJA37-79-C-0548), NTIS order No. AD-A087 610/2.

Cundall PA. Formulation of a three-dimensional distinct element model. *International Journal of Rock Mechanics, Mineral Sciences and Geomechanics* 1988; **25**: 107-16

Cundall, P. A. and Hart, R. D. (1985), Development of generalized 2D and 3D distinct element programs for modeling jointed rock, Misc. Paper SL-85-1, US Army Corps of Engineers, SL-85-1.

Cundall, P. A. and Hart, D. H. (1992), Numerical modeling of discontinua, *Eng. Comput.,* **9**, 101-113.

Cundall PA, Strack ODL. A discrete numerical model for granular assemblies. *Geotechnique* 1979; **29**: 47-65

Cleary, P. W. (1991), Extensions of the hybrid method for granular flows, Proceedings 5th International Computational Techniques and Applications Conference, Adelaide, Australia.

Cundall, P. A. (1980), UDEC-A generalized distinct element program for modeling jointed rock, Final Tech. Rep. Eur. Res. Office (US Army Contract DAJA37-79-C-0548), NTIS order No. AD-A087 610/2.

Ehlers W, Ramm E, Diebels S, D'Addetta GA. From particle ensembles to Cosserat continua: Homogenization of contact forces towards stresses and couple stresses. *International Journal of Solids and Structures* 2003; **40**: 6681-6702

Hart, R., Cundall, P. A., and Lemos, J. (1988), Formulation of a three-dimesional distinct element model - Part II. Mechanical calculations for motion and interaction of a system composed of many polyhedral blocks, *Int. J. Rock Mech. Min. Sci. Geomech. Abstr.,* **25**, 117-125.

Herbst JA, Potapov AV. Making a Discrete Grain Breakage model practical for comminution equipment performance simulation. *Powder Technology* 2004; **143-144**: 144-150

Heuze FE, *An overview of projectile penetration into geological materials, with emphasis on rocks*, D. o. Energy, 'Editor'. 1989, Lawrence Livermore National Laboratory

Jensen RP, Preece DS, *Modeling sand production with darcy-flow coupled with discrete elements*, in *Sandia National Laboratories Reports*. 2000, Sandia National Laboratories: Albuquerque, NM

Klosek JT, *The Integration of Fluid Dynamics with a Discrete-Element Modelling System: Algorithms, Implementation, and Applications*, in *Department of Civil and Environmental Engineering*. 1997, Massachusetts Institute of Technology: Cambridge, MA. 103.

Komodromos P, Williams JR. *On the simulation of deformable bodies using combined discrete and finite element methods*. in *Discrete Element Methods: Numerical Modeling of Discontinua*. 2002. Santa Fe, NM, USA: ASCE.

Kumano A, Goldsmith W. Behavior of diorite under impact by variously-shaped projectiles. *Rock Mechanics* 1982; **15**: 25-40

Kumano A, Goldsmith W. Analytical and experimental investigation of the effect of impact on coarse granular rocks. *Rock Mechanics* 1982; **15**: 67-97

Luding S. *About contact force-laws for cohesive frictional materials in 2D and 3D*. in *Behavior of Granular Media*. 2006.

Monaghan JJ. Smoothed particle hydrodynamics. *Annual Reviews of Astronomy and Astrophysics* 1992; **30**: 543-574

Morris, JP. Review of Rock Joint Models, Lawrence Livermore National Laboratory, UCRL-ID-153650, 2003. See http://www-r.llnl.gov/tid/lof/documents/pdf/244645.pdf.

Morris JP, et al. Simulations of underground structures subjected to dynamic loading using the distinct element method. *Engineering Computations* 2003; **21**: 348-408

Morris, JP, Rubin, MB, Block, GI, Bonner, MP, "Simulations of Fracture and Fragmentation of Geologic Materials using Combined FEM/DEM Analysis," International Journal of Impact Engineering, 33 (1-12): 463-473, 2006

Morris JP, Glenn LA, Heuze FE, Blair SC. *Simulations of underground structures subjected to dynamic loading using the distinct element method*. in *Proceedings of the Third International Conference on Discrete Element Methods; Numerical Modeling of Discontinua, Sep 23-25 2002*. 2002. Santa Fe, NM, United States: American Society of Civil Engineers.

Morris JP, Johnson SM. *Simulations of fracture and fragmentation of geologic materials using combined FEM/DEM/SPH analysis*. in *Discrete Element Methods 2007*. 2007. Brisbane, Australia.

Munjiza A, Bicanic N, Owen DRJ. *BSD contact detection algorithm for discrete elements in 2D*. in *Proceedings of the Second International Conference on Discrete Element Methods (DEM)*. 1993. Cambridge, MA, USA: AFOSR.

Munjiza A, Andrews KRF. NBS contact detection algorithm for bodies of similar size. *International Journal for Numerical Methods in Engineering* 1998; **43**: 131-149

Munjiza A, *The combined finite-discrete element method*. First ed. John Wiley & Sons: Chichester, West Sussex, England, 2004;333

Munjiza A, Andrews KRF. Penalty function method for combined finite-discrete element systems comprising large numbers of separate bodies. *International Journal for Numerical Methods in Engineering* 2000; **49**: 1377-1396

Munjiza A, Latham JP. *Computational challenge of large scale discontinua analysis*. in *Discrete Element Methods: Numerical Modeling of Discontinua*. 2002. Santa Fe, NM, USA: ASCE.

Munjiza A, Latham JP, Andrews KRF. Detonation gas model for combined finite-discrete element simulation of fracture and fragmentation. *International Journal for Numerical Methods in Engineering* 2000; **49**: 1495-1520

O'Connor RM, Friedrich J. Microscale flow modeling in geologic materials. *Physics and Chemisty of the Earth (A)* 1999; **24**: 611-616

Owen DRJ, Feng YT, Cottrel MG, Ju J. *Discrete/Finite element modeling of industrial applications with multi-fracturing and particulate phenomena*. in *Discrete Element Methods: Numerical Modeling of Discontinua*. 2002. Santa Fe, NM, USA: ASCE.

Nadler B, Rubin M. A new 3-D finite element for nonlinear elasticity using the theory of a Cosserat point. *International Journal of Solids and Structures* 2003; **40**: 4585-4614

Nelson RB, et al., *Numerical analysis of projectile penetration into boulder screens*, U. S. A. C. o. Engineers, 'Editor'. 1983, U.S. Army Engineer Waterways Experiment Station: Vicksburg, Mississippi, United States

Pentland A, Williams JR. Good vibrations: modal dynamics for graphics and animation. *Computer Graphics* 1989; **23**: 215-222

Perkins ED, Williams JR. *Generalized spatial binning of bodies of different sizes*. in *Discrete Element Methods: Numerical Modeling of Discontinua*. 2002. Santa Fe, NM, USA: ASCE.

Perkins ED, Williams JR. A fast contact detection algorithm insensitive to object sizes. *Engineering Computations* 2001; **18**: 48-61

Potapov AV, Hunt ML, Campbell CS. Liquid–solid flows using smoothed particle hydrodynamics and the discrete element method. *Powder Technology* 2001; **116**: 204-13

Preece DS, Jensen RP, Perkins ED, Williams JR. *Sand production modeling using superquadric discrete elements and coupling of fluid flow and particle motion*. in *Rock Mechanics for Industry: Proceedings of the 37th U.S. Symposium*. 1999. Vail, Colorado: Taylor and Francis.

Rougier E, Munjiza A, John NWN, *Numerical comparison of some explicit time integration schemes used in DEM, FEM/DEM and molecular dynamics*. 2004. 856-879.

Rubin M. Numerical solution procedures for nonlinear elastic rods using the theory of the Cosserat point. *International Journal of Solids and Structures* 2001; **38**: 4395-4437

Rubin M, Morris JP, Johnson SM, *Stress, strain and failure of a "rigid" body in motion using the theory of a Cosserat point*, in *Internal report*. 2006, Lawrence Livermore National Laboratory: Livermore, California. 29.

M. Souley. An extention to the saeb and amadei constitutive model for rock joints to include cyclic loading paths. *Int. J. Rock Mech. Min. Sci. & Geomech. Abstr.*, 32(2):101.109, 1995.

Walton, O. R. (1980), Particle dynamics modeling of geological materials, Lawrence Livermore National Laboratory, UCRL-52915.

Walton OR. *Force models for particle dynamics simulations of granular materials*. in *NATO ASI Symposium*. 1994. Corsege, Corsica: Kluwer Academic Publishers.

Williams JR, Hocking G, Mustoe GGW. *The theoretical basis of the discrete element method*. in *NUMETA*. 1985. Swansea, UK.

Williams JR, O'Connor RM. A linear complexity intersection algorithm for discrete element simulation of arbitrary geometries. *International Journal for Numerical and Analytical Methods in Geomechanics* 1995; **12**: 185-201

Williams JR, Mustoe GGW. Modal methods for the analysis of discrete systems. *Computers and Geotechnics* 1987; **4**: 1-19